Bull. Mater. Sci., Vol. 37, No. 6, October 2014, pp. 1301–1308. © Indian Academy of Sciences.

Optimization of process conditions for the production of $TiO_{2-x}N_y$ film by sol–gel process using response surface methodology

RUI LIU[a], CHING-SHIEH HSIEH[b], WEIN-DUO YANG[c,]* and HUI-YI TSAI[c]

[a]Institute of Petroleum and Commodity, Harbin University of Commerce, Harbin 150076, China
[b]Department of Applied Chemistry, Fooyin University, Ta-Liao 831, Taiwan
[c]Department of Chemical and Materials Engineering, National Kaohsiung University of Applied Sciences, Kaohsiung 807, Taiwan

MS received 3 June 2013

Abstract. **$TiO_{2-x}N_y$ film has been synthesized successfully through the sol–gel method. It is found that the anatase phase is formed at 400 °C and converted to rutile phase at 600 °C. The response surface methodology (RSM) and Box–Behnken design were employed to optimize the process conditions of sol–gel process. Based on the results in preliminary experiments, we selected molar ratio of surfactant to Ti, molar ratio of acetylacetone to Ti, molar ratio of water to Ti and calcination temperature as the key process factors affecting the roughness of $TiO_{2-x}N_y$ film. The adjusted determination coefficient (R^2_{Adj}) of the regression model was 0·9651, which indicated that the regression model is significant. By analysing the contour plots of response surface as well as solving the regression model, the optimized conditions were obtained as: 0·19 for molar ratio of surfactant to Ti, 2·01 for molar ratio of acetylacetone to Ti, 1·38 for molar ratio of water to Ti and 500 °C for calcination temperature. The predicted roughness of $TiO_{2-x}N_y$ film for the optimized condition was calculated to be 41 nm. Confirmation experiments using the optimized conditions were performed, and a value about 43 nm was obtained. The experimental results are in good agreement with the predicted results.**

Keywords. **Titania; $TiO_{2-x}N_y$ film; sol–gel method; Box–Behnken design.**

1. Introduction

TiO_2 is an important functional inorganic material due to good stability, strong oxidizing power, low cost and non-toxicity (Sreekantan *et al* 2009). Anatase, brookite and rutile were examined as three crystalline forms of titania. TiO_2 is amorphous but crystallized with annealing at a certain temperature. Rutile phase is the most stable among three forms. Anatase and brookite are metastable, and transformed to rutile by a heating process. TiO_2 as a semiconductor has excellent photo-catalytical properties, which can be excited by ultraviolet light (Fujishima and Honda 1972; Linsebigler *et al* 1995). Most scholars (Asahi *et al* 2001; Irie *et al* 2003; Lindgren *et al* 2003; Shankar *et al* 2006; Vitiello *et al* 2006) have found that N-doping is the most promising path towards photo-catalytical applications. Nitrogen ions substituted oxygen atoms in the TiO_2 lattice and, thus, the band-gap energy is narrower compared with TiO_2. As a result, higher photo-electrochemical efficiencies can be obtained.

There are a variety of techniques available for preparing thin films, such as hydrothermal processing (Yang and Hung 2002), sol–gel process (So *et al* 2001), aqueous precipitation (Yuan *et al* 2006) and gas-phase reaction (Nakamura *et al* 2000). Among the various methods, films obtained by the sol–gel are the realizable method because of low cost, simple and safe preparation technology. However, original materials such as $Ti(OR)_4$ in sol–gel method are apt to hydrolyze, leading to formation of non-uniform chemical composition. To overcome this drawback, acetylacetone (Selvaraj *et al* 1994; Algueró *et al* 1999; Moon *et al* 2002) is used as chelating agent with titanium alkoxides, since it significantly changes the hydrolysis behaviours as a nucleophilic reactant in preparation process.

Box–Behnken design (Morgenthaler and Schumacher 1999; Hsieh and Liou 2001) is an independent quadratic design which does not contain an embedded factorial or fractional factorial design. These designs are rotatable (or near rotatable) and require 3 levels of each factor. Box–Behnken design is also a spherical design, with all points lying on a sphere of radius $\sqrt{2}$. Also, Box–Behnken design does not contain any points at the vertices of the cubic region created by the upper and lower limits for each factor. This can be advantageous when the points on the corners of the cube represent factor-level combinations that are prohibitively expensive or impossible to test because of physical process constraints.

*Author for correspondence (ywd@cc.kuas.edu.tw)

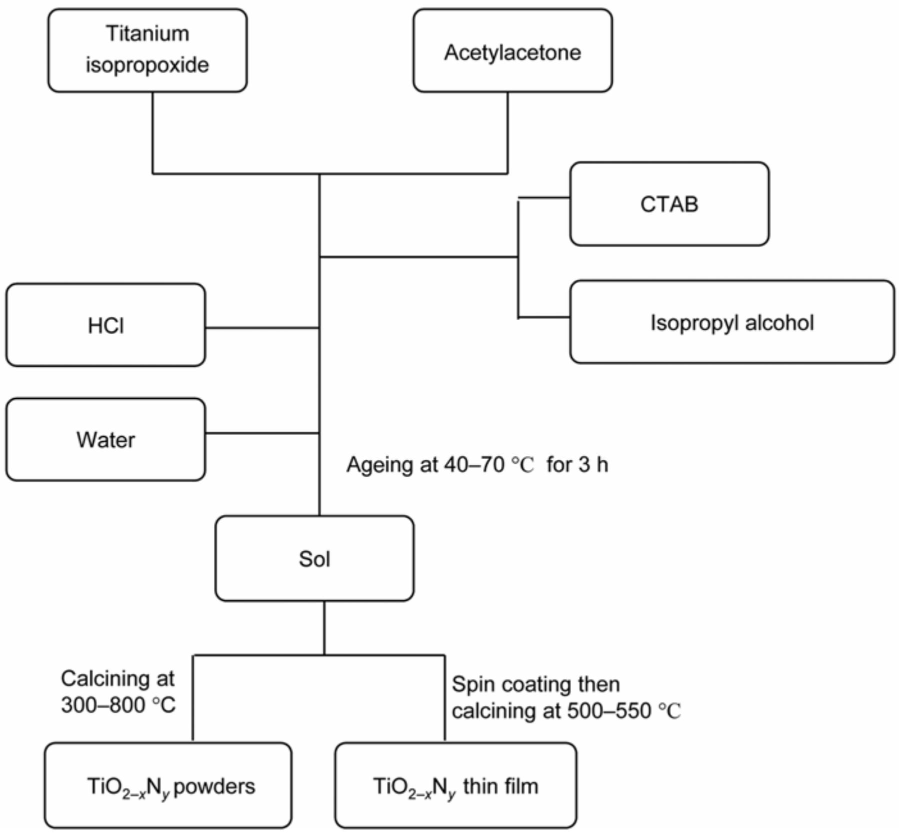

Figure 1. Schematic illustration of the preparation of $TiO_{2-x}N_y$ film from sol–gel method.

Experimental statistical methods are often used in the design experiments and the significant factors of the preparatory conditions. This is also an effective method to simplify the process of identifying the most influential preparation variables. However, there have been few studies to investigate the optimization of experimental conditions in the preparation of $TiO_{2-x}N_y$ film by sol–gel method.

This study applied Box–Behnken design and response surface methodology (RSM) to obtain the optimal conditions for preparation of $TiO_{2-x}N_y$ films by sol–gel method. Based on Box–Behnken design with three factors, a set of 29 experiments was carried out. The statistical software package Design–Expert (Version 7.1.4, Stat-ease Inc., Minneapolis, MN, USA) was used to analyse the experimental results.

2. Experimental

2.1 *Synthesis of $TiO_{2-x}N_y$ films*

Titanium isopropoxide ($Ti(O–i–C_3H_7)_4$, density 0·995 g cm^{-1}, purity 98%) was reacted with acetylacetone to obtain a Ti-acetylacetonate precursor. Isopropyl alcohol was applied for solvent, and hexadecyltrimethylammonium bromide (CTAB) of surfactant used as template. In the reaction, water and hydrochloric acid were added to the mixture, and stirred vigorously. To determine the crystal phase, the samples were heated at 300–800 °C at normal atmospherical condition to produce yellowish powders. To obtain $TiO_{2-x}N_y$ film, the $TiO_{2-x}N_y$ coating was formed on the glass substrate by a dip-coating method, and then the samples were calcinated at 500–550 °C for 3 h. A schematic diagram for the preparation of $TiO_{2-x}N_y$ film by the sol–gel method is shown in figure 1.

2.2 *Optimization by response surface methodology*

Response surface methodology (RSM) (Myers and Montgomery 1995; Montgomery 2001) is an empirical modeling technique used to construct the relationships between controllable process factors and response variables. RSM can be used extensively for developing, improving and optimizing processes. The process factors' molar ratio of surfactant to Ti, molar ratio of acetylacetone to Ti, molar ratio of water to Ti and calcination temperature were chosen as the key factors and assigned as x_1, x_2, x_3 and x_4, respectively. Box–Behnken design (Box and Behnken 1960; Box and Draper 1987) with four factors and RSM were employed to find the optimized conditions

Table 1. The actual and code levels of factors for Box–Behnken design.

Factors	Coded levels		
	–1	0	+ 1
x_1: molar ratio of surfactant to Ti	0·05	0·15	0·25
x_2: molar ratio of acetylacetone to Ti	2	3	4
x_3: molar ratio of water to Ti	1	3	5
x_4: calcination temperature, °C	500	525	550

of the process factors within the observed region. Each factor was assigned three levels at low level (–1), middle level (0) and high level (+1), as shown in table 1. The central values (zero level) chosen for experimental design are molar ratio of surfactant to Ti (x_1) = 0·15, molar ratio of acetylacetone to Ti (x_2) = 3, molar ratio of water to Ti (x_3) = 3 and calcination temperature (x_4) = 525 °C. Based on Box–Behnken design with four factors, a set of 29 experiments was carried out.

In developing the regression model, the process factors were coded according to the following equation

$$x_i = \frac{X_i - X_0}{\Delta X_i}, \tag{1}$$

where x_i is the coded variable of the ith process factor, X_i the actual variable of the ith process factor, X_0 the actual value of the ith process factor at the central point and ΔX the step change value.

According to the RSM, a full second-order polynomial model was used to fit the experimental results using the following equation

$$\begin{aligned} Y = {} & b_0 + b_1x_1 + b_2x_2 + b_3x_3 + b_4x_4 + b_{11}x_1^2 \\ & + b_{22}x_2^2 + b_{33}x_3^2 + b_{44}x_4^2 + b_{12}x_1x_2 + b_{13}x_1x_3 \\ & + b_{14}x_1x_4 + b_{23}x_2x_3 + b_{24}x_2x_4 + b_{34}x_3x_4, \end{aligned} \tag{2}$$

where Y is the roughness of $TiO_{2-x}N_y$ film (nm), b_i the coefficients of the model, x_1 the coded variable of molar ratio of surfactant to Ti, x_2 the coded variable of molar ratio of acetylacetone to Ti, x_3 the coded variable of molar ratio of water to Ti and x_4 is the coded variable of calcination temperature. The obtained regression model can be used for prediction, process optimization and process control.

2.3 *Characterization analysis*

The crystal phases of the $TiO_{2-x}N_y$ were investigated by X-ray diffraction (PANalytical/X'Pert PRO MPD) using CuKα (λ = 0·154 nm) ranging from 20 to 80°, with a working condition of 10 kV, 100 mA. The morphologies of the samples were investigated by a field emission scanning electron microscope (FESEM, JEOL JSM-7401F) at 5 kV. The surface roughness was analysed by atomic force microscopy (BASO–AFM). X-ray photoelectron spectroscopy (XPS, Kratos Axis Ultra DLD) patterns were obtained using a monochromatic Al-anode X-ray gun.

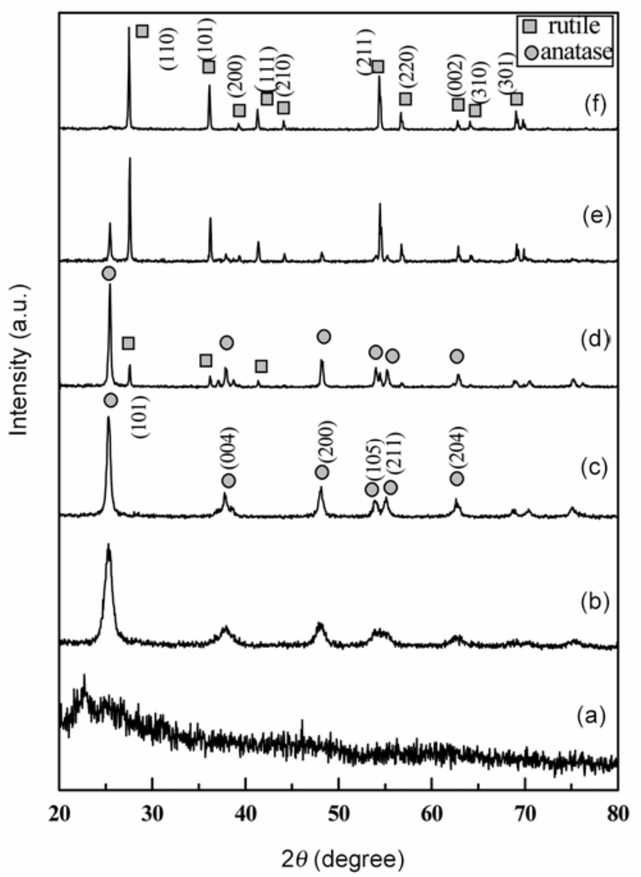

Figure 2. XRD patterns of $TiO_{2-x}N_y$ calcined at various temperatures: (a) 300, (b) 400, (c) 500, (d) 600, (e) 700 and (f) 800 °C.

2.4 *Photo-catalytic measurements*

A reactor, irradiated by the light source placed above the methylene blue solution at a certain position, was utilized to perform the photo-catalytic experiments. The volume of the reactor was 250 mL. A 369 nm UV lamp was used as the light source and 1 × 1 mm^2 of $TiO_{2-x}N_y$ film was putted into 50 mL of 9 ppm methylene blue solution to

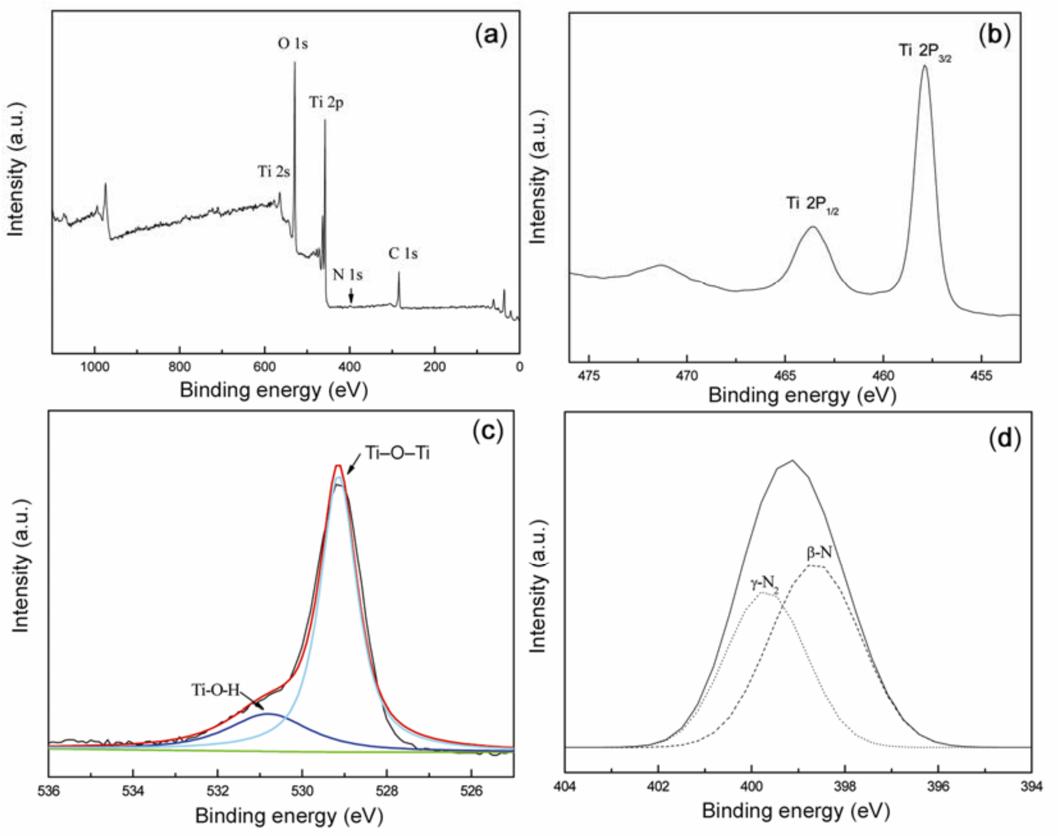

Figure 3. XPS spectra of $TiO_{2-x}N_y$ film: (**a**) full spectrum, (**b**) high resolution of Ti 2*p*, (**c**) high resolution of O 1*s* and (**d**) high resolution of O 1*s*.

measure the photodegradation activity of as-prepared photo-catalyst. The photodegradation runs lasted several hours and samples were taken for examination during the interval of degradation. The concentration of methylene blue was measured at the maximum absorption wavelength of 664 nm by a HITACHIU-2800 UV–Vis spectrophotometer.

3. Results and discussion

3.1 *Characteristics of $TiO_{2-x}N_y$ film*

The XRD patterns of $TiO_{2-x}N_y$ were determined by X-ray diffraction with annealing at different temperatures for 3 h, as shown in figure 2, in which A and R stood for anatase and rutile, respectively (ratio of surfactant to Ti = 0·0625 : 1, molar ratio of acetylacetone to Ti = 4 : 1). At 300 °C, $TiO_{2-x}N_y$ powders are amorphous and crystallized by high-temperature annealing. Anatase phase was found at a temperature of 400 °C, with the (1 0 1) and (2 0 0) characteristic peaks of anatase phase appearing at about 25° and 48°. With the increase of the annealing temperature to 500 °C, the obvious anatase crystal planes of (1 0 1), (0 0 4), (2 0 0), (1 0 5) and (2 0 4) are observed. Rutile phase began to appear at 600 °C, while the rutile (1 1 0) peak grew, the anatase (1 0 1) peak diminished with the temperature increased to 700 °C. When $TiO_{2-x}N_y$ powders were annealed at the temperature of 800 °C, the peak of the anatase phase vanished completely, which indicates that the crystallization of titanium thoroughly changed into rutile phase.

XPS was used to examine the elemental composition of $TiO_{2-x}N_y$ film. Ti, O and N elements were detected using full XPS spectra of $TiO_{2-x}N_y$ films, as shown in figure 3(a). Strong diffraction peaks at 457·9 and 463·5 eV are ascribed to Ti $2p_{3/2}$ and Ti $2p_{1/2}$ in high-resolution Ti (2*p*), which is a little different from previous reports (458·5 and 464·2 eV) (Yang *et al* 2004). That is because Ti–O–N bond has influence on the energy of Ti 2*p* due to N incorporation. The O1*s* XPS spectra having a peak at 529·1 and 530·8 eV are attributed to Ti–O–Ti and Ti–O–H, respectively, as shown in figure 3(c). The blue shift of $TiO_{2-x}N_y$ compared to TiO_2 (Jang *et al* 2000) is due to the formation N–O and Ti^{3+}–O. Figure 3(d) shows two peaks with the binding energies at 400 and 398 eV, assigned to γ-N_2 and atomic β-N, respectively (Saha and Tompkins 1992). Analysis obtained by Gaussian function shows that the intensity of the atomic β-N peak is stronger than γ-N_2 peak, which indicates most of nitrogen incorporated in the $TiO_{2-x}N_y$ films are atomic nitrogen. It is easy to desorb for γ-N_2, while the N atom in the lattice can supply electron to shorten the band gap for β-N.

3.2 *Optimization of the key factors*

The Box–Behnken design and experimental results were shown in table 2. The experimental results were analysed using Design–Expert. Multiple regression analysis of the experimental data gave the following second-order regress model

$$Y = 10.88 + 2.38x_1 - 1.73x_2 + 0.66x_3 - 4.59x_4 - 6.38x_1^2 + 7.99x_2^2 + 0.27x_3^2 + 4.57x_4^2 - 2.40x_1x_2 - 0.42x_1x_3 - 0.80x_1x_4 - 1.08x_2x_3 + 9.00x_2x_4 + 2.42x_3x_4, \quad (3)$$

where Y is roughness of the $TiO_{2-x}N_y$ film; x_1 molar ratio of surfactant to Ti; x_2 the molar ratio of acetylacetone to Ti; x_3 the molar ratio of water to Ti and x_4 the calcination temperature.

A summary of the analysis of variance (ANOVA) for the regress model is shown in table 3. The goodness of the fit of the regression model can be checked by the adjusted coefficient of determination R^2_{Adj}. The value of R^2_{Adj} for the regression model being close to 1 indicates a high degree of correlation between the observed and predicted values. The R^2_{Adj} of the model is 0·9651 (a value > 0·75 indicates aptness of the model), which means that the model can be expected to explain about 96·51% variation in the response. The $R^2_{\text{Predicted}}$ of the model is 0·9054, which means that the model can be expected to explain about 90·54% of the variation in predicting new observations. Statistical testing of the model was done in the form of ANOVA, which is required to test the significance and adequacy of the model. Here, the ANOVA of the regression model demonstrates that the model is highly significant, as is evident from the calculated F-value (56·31) and a very low probability value ($P < 0.0001$). Moreover, the computed F-value is much greater than the tabulated F-value ($F_{0.01}(14, 14) = 3.85$) indicating that the treatment differences are highly significant. The model also showed statistically insignificant lack of fit, as is evident from the lower calculated F-value (4·55) than the tabulated F-value ($F_{0.05}(14, 10) = 3.02$) even at 0·05 level. The model was found to be adequate for prediction within the range of variables employed.

Table 2. Box–Behnken design and responses.

Trial no.	x_1	x_2	x_3	x_4	Roughness (nm) Observed	Roughness (nm) Predicted
1	–1	–1	0	0	8·8	9·4
2	1	–1	0	0	19·8	19·0
3	–1	1	0	0	9·3	10·8
4	1	1	0	0	10·7	10·7
5	0	0	–1	–1	23·0	22·1
6	0	0	1	–1	18·5	18·5
7	0	0	–1	1	7·2	8·0
8	0	0	1	1	12·6	14·2
9	–1	0	0	–1	9·2	10·5
10	1	0	0	–1	15·5	16·8
11	–1	0	0	1	4·1	2·9
12	1	0	0	1	7·2	6·1
13	0	–1	–1	0	18·5	19·1
14	0	1	–1	0	16·2	17·8
15	0	–1	1	0	24·1	22·6
16	0	1	1	0	17·5	17·0
17	–1	0	–1	0	3·0	1·3
18	1	0	–1	0	7·2	6·9
19	–1	0	1	0	4·0	3·5
20	1	0	1	0	6·5	7·4
21	0	–1	0	–1	38·7	38·8
22	0	1	0	–1	19·1	17·3
23	0	–1	0	1	10·6	10·9
24	0	1	0	1	27·0	26·1
25	0	0	0	0	10·6	10·9
26	0	0	0	0	10·1	10·9
27	0	0	0	0	11·9	10·9
28	0	0	0	0	10·3	10·9
29	0	0	0	0	11·1	10·9

The coefficient values were tested for their significance using Design Expert; and are listed in table 4. The P values are used as a tool to check the significance of each of coefficients, which in turn may indicate the pattern of the interactions between the variables. The smaller the value of P, the more significant is the corresponding coefficient. It can be seen from this table that the linear terms (x_1, x_2, x_4), the quadratic terms (x_1^2, x_2^2, x_4^2) and the interaction terms (x_1x_2, x_2x_4, x_3x_4) are statistically significant, the P values being very small ($P < 0.01$).

The regression model can be used for prediction, process optimization and process control. Comparisons of experimental values and predicted values from the regression model are shown in table 5. It is observed that the experimental values are in good agreement with the predicted values. According to the regression model, the optimized conditions of process factors can be searched to maximize the roughness of $TiO_{2-x}N_y$ film by using Design Expert. The optimized conditions of the process factors are 0·19 for molar ratio of surfactant to Ti (x_1), 2·01 for molar ratio of acetylacetone to Ti (x_2), 1·38 for molar ratio of water to Ti (x_3) and 500 °C for calcination temperature (x_4). Viewing the contour plot of the response surface shown in figure 4, the optimized conditions can be checked too. Corresponding to the actual variable, the optimized conditions are 0·19 for molar ratio of surfactant to Ti (x_1), 2·01 for molar ratio of acetylacetone to Ti (x_2), 1·38 for molar ratio of water to Ti (x_3), and 500 °C for calcination temperature (x_4). The predicted roughness of $TiO_{2-x}N_y$ film for the optimized condition was calculated to be about 41 nm. In order to confirm the predicted

Table 3. ANOVA for regression model.

Source	Sum of squares	Degree of freedom	Mean square	F_0	P-value
Model	1704·40	14	121·74	56·31	< 0·0001
Lack of fit	27·82	10	2·78	4·55	0·0788
Residual	30·27	14	2·16		
Total	1734·67	28			

$R^2 = 0{\cdot}9826$, $R^2_{\text{Adj}} = 0{\cdot}9651$, $R^2_{\text{Predicted}} = 0{\cdot}9054$.

Table 4. Test of significance for regression coefficients.

Model term	Coefficient estimate	Degree of freedom	S.E.	95% CI low	95% CI high	P-value
Intercept	10·88	1	0·66	9·47	12·29	
x_1	2·38	1	0·42	1·46	3·29	< 0·0001
x_2	–1·73	1	0·42	–2·64	–0·81	0·0012
x_3	0·66	1	0·42	–0·25	1·57	0·1432
x_4	–4·59	1	0·42	–5·50	–3·68	< 0·0001
x_1^2	–6·38	1	0·58	–7·62	–5·14	< 0·0001
x_2^2	7·99	1	0·58	6·76	9·23	< 0·0001
x_3^2	0·27	1	0·58	–0·97	1·51	0·6492
x_3^2	4·57	1	0·58	3·33	5·81	< 0·0001
x_1x_2	–2·40	1	0·74	–3·98	–0·82	0·0056
x_1x_3	–0·42	1	0·74	–2·00	1·15	0·5724
x_1x_4	–0·80	1	0·74	–2·38	0·78	0·2949
x_2x_3	–1·08	1	0·74	–2·65	0·50	0·1658
x_2x_4	9·00	1	0·74	7·42	10·58	< 0·0001
x_3x_4	2·42	1	0·74	0·85	4·00	0·0053

Table 5. The optimized conditions for $TiO_{2-x}N_y$ film.

Factor	Optimal conditions	Predicted	Observed
A: molar ratio of CTAB/$Ti(OR)_4$	0·19	41 nm	43 nm
B: molar ratio of AcAc/$Ti(OR)_4$	2·01		
C: molar ratio of water/$Ti(OR)_4$	1·38		
D: calcination temperature (°C)	500		

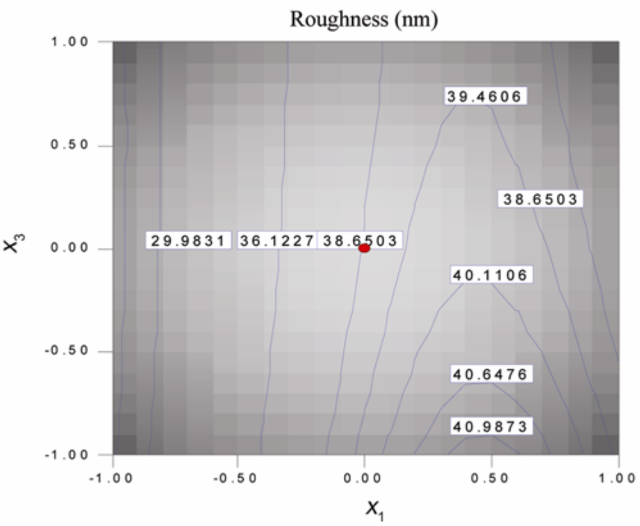

Figure 4. The contour plot of overall desirability.

results, experiments using the optimized conditions were performed, and a value about 43 nm was observed. The FESEM and AFM micrographs of the $TiO_{2-x}N_y$ film at optimized conditions are represented in figure 5. The roughness of $TiO_{2-x}N_y$ film is 43 nm by AFM analysis, and the thickness of $TiO_{2-x}N_y$ film is 140·6 nm.

3.3 *Photo-catalytic activity of $TiO_{2-x}N_y$ film*

The concentration of methylene blue was determined by a UV–Vis spectrophotometer. The photo-catalytic decolorization of methylene blue is a first-order reaction and its kinetics can be expressed as followed (Syoufian and Nakashima 2007)

$$\ln \frac{C}{C_0} = -kt, \tag{4}$$

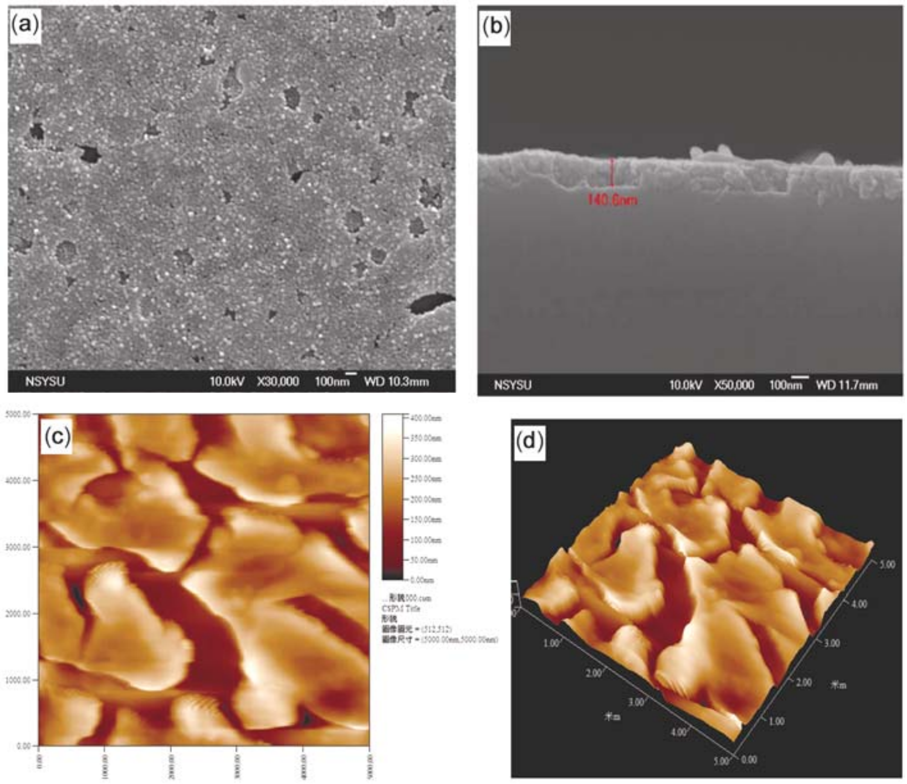

Figure 5. FESEM and AFM micrographs of $TiO_{2-x}N_y$ film at optimized conditions: (**a**) top and (**b**) cross-sectional view of FE–SEM, (**c**) two-dimensional and (**d**) three-dimensional micrographs of AFM.

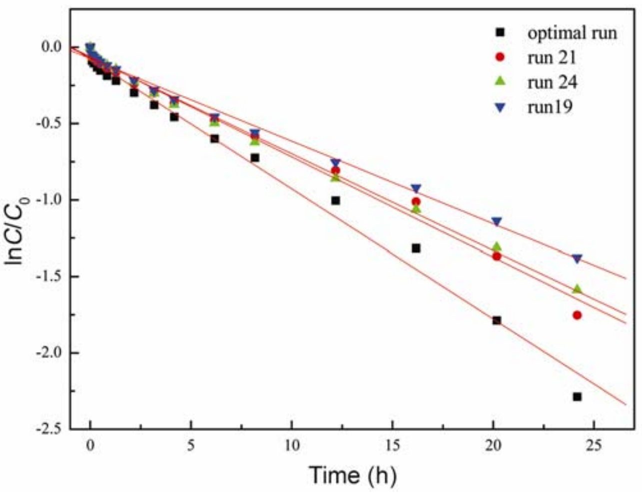

Figure 6. The photodegradation reaction rate of methylene blue by the as-prepared $TiO_{2-x}N_y$ film obtained from run 21, run 24, run 19 and the optimal experiment.

where k is the apparent reaction rate constant, C_0 and C are the initial concentration and the reaction concentration of methylene blue, respectively.

The photodegradation reaction rate of methylene blue by $TiO_{2-x}N_y$ film obtained from run 21, run 24, run 19 and the optimal experiment were measured as shown in figure 6. The apparent reactant rate constants are $1{\cdot}10 \times 10^{-3}$, $1{\cdot}05 \times 10^{-3}$, $0{\cdot}90 \times 10^{-3}$ and $1{\cdot}42 \times 10^{-3}$ min^{-1}, respectively. Clearly, the apparent rate constants depend on the roughness of $TiO_{2-x}N_y$ film. The rate constant increases with increasing roughness in expectation.

4. Conclusions

$TiO_{2-x}N_y$ film has been synthesized successfully by sol–gel method. The selected experimental factors were molar ratio of surfactant to Ti, molar ratio of acetylacetone to Ti, molar ratio of water to Ti and calcination temperature for the optimal experiment. Based on the XRD analysis, it is apparent from the results that anatase phase is formed completely at 500 °C and complete conversion into rutile occurs at 800 °C. Furthermore, Box–Behnken design with key factors and RSM were employed to find the optimized conditions of the process factors. A regression model for the roughness of $TiO_{2-x}N_y$ film was established as a function of the key factors. The adequacy and lack of fit of the regression model were verified significantly by the validation data. Based on the regression model, it reveals that the optimal preparatory conditions were obtained at molar ratio of surfactant to Ti = 0·19, molar ratio of acetylacetone to Ti = 2·01, molar ratio of water to Ti = 1·38, calcination temperature = 500 °C.

Corresponding to the optimized conditions, the predicted and the observed values of the roughness of film were in good agreement. Finally, photo-catalytic degradation experiments were examined and they demonstrated that methylene blue remarkably enhanced the degradation in the presence of $TiO_{2-x}N_y$ film prepared from the optimal conditions under ultraviolet light.

References

Algueró M, Calzada M L, Quintana C and Pardo L 1999 *Appl. Phys.* **A68** 583

Asahi R, Morikawa T, Ohwaki T, Aoki K and Taga Y 2001 *Science* **293** 269

Box G E P and Behnken D W 1960 *Technometrics* **2** 455

Box G E P and Draper N R 1987 *Empirical model-building and response surfaces* (New York: John Wiley & Sons)

Fujishima A and Honda K 1972 *Nature* **238** 37

Hsieh C S and Liou T S 2001 *Qual. Eng.* **13** 449

Irie H, Watanabe Y and Hashimoto K 2003 *J. Phys. Chem.* **B107** 5483

Jang H K, Whangbo S W, Kim H B, Im K Y, Lee Y S, Lyo I W, Whang C N, Kim G, Lee H S and Lee J M 2000 *J. Vac. Sci. Technol., A, Vac. Surf. Films* **18** 917

Lindgren T, Mwabora J M, Avendano E and Jonsson J 2003 *J. Phys. Chem.* **B107** 5709

Linsebigler A L, Lu G Q and Yates J T 1995 *Chem. Rev.* **95** 735

Montgomery D C 2001 (New York: John Wiley & Sons)

Moon J, Suvaci E, Li T, Costantino A and Adair J H 2002 *J. Eur. Ceram. Soc.* **22** 809

Morgenthaler S and Schumacher M M 1999 *Chemom. Intell. Lab. Syst.* **47** 127

Myers R H and Montgomery D C 1995 Response surface methodology: process and product optimization using designed experiments (New York: John Wiley & Sons)

Nakamura I, Negishi N, Kutsuna S, Ihara T, Sugihara S and Takeuchi K 2000 *J. Mol. Catal. A: Chem.* **161** 205

Saha N C and Tompkins H G 1992 *J. Appl. Phys.* **72** 3072

Selvaraj U, Prasadarao A V and Komarneni S 1994 *Mater. Lett.* **20** 71

Shankar K, Tep K C, Mor G K and Grimes C A 2006 *J. Phys. D: Appl. Phys.* **39** 2361

So W W, Park S B, Kim K J, Shin C H and Moon S J 2001 *J. Mater. Sci.* **36** 4299

Sreekantan S, Hazan R and Lockman Z 2009 *Thin Solid Films* **518** 16

Syoufian A and Nakashima K 2007 *J. Coll. Interf. Sci.* **313** 213

Vitiello R P, Macak J M, Ghicov A and Tsuchiya H 2006 *Electrochem. Commun.* **8** 544

Yang W D and Hung K M 2002 *J. Mater. Sci.* **37** 1337

Yang T S, Shu C B and Wong M S 2004 *Surf. Sci.* **548** 75

Yuan J, Chen M, Shi J and Shangguan W 2006 *Int. J. Hydrogen Energy* **31** 1326